KFUPM
Journal of Undergraduate Research International

Diamond Open Access

Article *XXXXX*

Artificial Neural Networks for Predicting the Maximum Surface Settlement Induced by EPB-TBM: The Algiers Metro Case

Ilies AYARI[1], and Yacine DERBAL[2]

Cite https://doi.org/10.0000/0.0000000

Submitted: XXXX 00, 0000 **Revised:** XXXX 00, 0000 **Accepted:** XXXX 00, 0000

ABSTRACT

Surface settlement poses a risk to nearby structures, utilities, and cultural heritage sites. This paper presents the development of an Artificial Neural Network (ANN) model for predicting the maximum surface settlement induced by Earth Pressure Balance Tunnel Boring Machines (EPB-TBMs) with a specific application to the Algiers Metro Line 1 extension. The model was trained on a dataset comprising 442 samples incorporating operational parameters, geometric characteristics, and geotechnical data. Following a structured preprocessing phase, the ANN achieved high predictive performance, with coefficients of determination (R^2) exceeding 0.92 and a root mean square error (RMSE) below 4.2 mm. Compared to the Random Forest and XGBoost models, which yielded R^2 values of 0.679 and 0.7859, respectively, and exhibited higher RMSEs, demonstrating superior capability in capturing complex nonlinear relationships, the ANN demonstrated superior performance in capturing nonlinear relationships. Sensitivity analysis identified the equivalent cover depth, groundwater head, and distance from the station as the most influential variables. These results demonstrate that the ANN model can significantly enhance real-time decision-making in urban tunneling projects, contributing to more accurate settlement predictions and ultimately reducing risks to surrounding infrastructure and public safety.

Keywords: Artificial neural network, EPB-TBM Tunneling, prediction of surface settlement, machine learning.

1. INTRODUCTION

The rapid expansion of urban areas has intensified the need for efficient underground infrastructure, particularly metro systems, to alleviate surface congestion and improve mobility. However, the construction of tunnels in dense city environments presents significant geotechnical challenges, particularly when excavations occur at shallow depths in heterogeneous soils. A primary concern during mechanized tunneling is ground surface settlement, which can jeopardize nearby structures, utilities, and cultural heritage sites. This is especially critical in cities such as Algiers, where historical and archaeological sensitivities add further complexity to underground works [1]. Mechanized tunneling using EPB-TBMs has emerged as the preferred solution in such settings because of its ability to maintain face stability on soft ground. However, despite technological advances, ground movement remains inevitable. Therefore, the accurate prediction of surface settlement is vital for optimizing TBM control, safeguarding infrastructure, and guiding real-time decision-making during excavation.

Over the past decades, a wide range of approaches has been developed to estimate tunneling-induced ground settlement. Traditional methods include empirical techniques based on Gaussian distribution models (e.g., Peck, 1969), stochastic risk models, and semi-analytical solutions derived from cavity expansion and elasticity theory. Although computationally efficient, these models often oversimplify subsurface behavior and fail to account for real-time operational parameters. More sophisticated techniques, such as the finite element method (FEM) and finite difference method (FDM), allow for the detailed simulation of ground–structure interactions with higher spatial resolution. However, they typically require significant calibration, are highly sensitive to boundary conditions and mesh configurations, and are computationally demanding, rendering them unsuitable for real-time tunnel control applications. Although theoretically robust, these models rely on idealized assumptions and intensive parameter tuning, which limit their practical utility in dynamic, data-rich tunneling scenarios [2]. Recent advances in ANN-based frameworks, including operator-learning networks for fusing simulation and monitoring data [3], and AI-driven prediction pipelines tailored to shield tunneling operations [4], demonstrate significant potential to overcome these challenges by providing rapid, accurate settlement forecasts under actual tunneling conditions. To address these challenges, data-driven models have recently attracted considerable attention. Ensemble methods such as Random Forest and XGBoost have demonstrated strong performance in geotechnical regression tasks5. However, these models rely on hierarchical decision-tree logic and may struggle to capture the complex interdependencies among the input features4. In contrast, artificial neural networks (ANNs) offer a robust solution for modeling nonlinear and multivariate relationships, and are particularly well-suited for problems involving diverse geotechnical and operational variables. Several studies, such as those by Suwansawat and Einstein (2006)[6] and Boubou et al. (2015)[7], successfully applied ANN models to tunneling-induced settlement predictions across a variety of geological and project-specific contexts.

Despite being a well-established method, ANNs continue to be widely adopted because of their practical balance between predictive accuracy, computational efficiency, and interpretability[8]. Although deep learning architectures such as a convolutional neural network (CNN) and recurrent neural network (RNN) offer greater representational capacity, their use in tunneling remains limited. These models typically require large, high-resolution datasets and extended training times, and often function as "black boxes" with low transparency[9,10]. Deep learning is gaining traction in geotechnical engineering[11]. The ANN remains the dominant and most trusted machine learning method for ground surface settlement prediction because of its lower data demands, greater interpretability, and strong empirical record[12]. In tunneling projects such as the Algiers Metro Line 1 extension, where historical and operational data are valuable but moderately sized, shallow feedforward ANNs offer a practical and robust solution. They are easier to train and less prone to overfitting, and when combined with sensitivity analysis, they can provide interpretable insights into feature influence, supporting informed engineering decisions during excavation.

This study aims to develop and evaluate an ANN-based predictive model for estimating the maximum surface settlement induced by EPB-TBM tunneling using real-world data from the Algiers Metro Line 1 extension project. The dataset integrates operational parameters (e.g., thrust and face pressure), geometrical indicators (e.g., equivalent cover depth and distance from stations), and geotechnical variables (e.g., groundwater head and Em/pl ratio). The ANN performance was benchmarked against Random Forest and XGBoost to assess the predictive accuracy and generalization capacity. Sensitivity analyses (based on perturbation and weight-based techniques) were conducted to interpret the influence of each input feature on the predicted settlement. The findings aim to deliver a scalable, interpretable, and accurate decision-support tool for real-time risk management in mechanized urban tunneling.

The remainder of this study is structured as follows.

- **Section 2** presents the background and dataset characteristics of the Algiers metro project.
- **Section 3** Details the Neural network methodology and model development process.
- **Section 4** reports the model performance, a comparison with alternative methods, and sensitivity analysis results.
- **Section 5** discusses the findings.
- **Section 6** outlines the key conclusions.

2. PROJECT DESCRIPTION AND DATASET CONSTRUCTION

2.1. Project Overview. The dataset used for this research was obtained from completed construction works of the Algiers Metro Line 1 extension project connecting the El Harrach Centre to Houari Boumédiène International Airport. The excavation was conducted using an EPB-TBM across 9,565 m, segmented into 10 main tunnel sections. The project involved tunneling through highly variable soil conditions, including alluvial deposits, clayey sands, marls, and conglomerates, under varying groundwater conditions. The metro line extension project was conducted in two main phases (Fig. 2.2). Oued–Smar as a Launch and Supply Section.

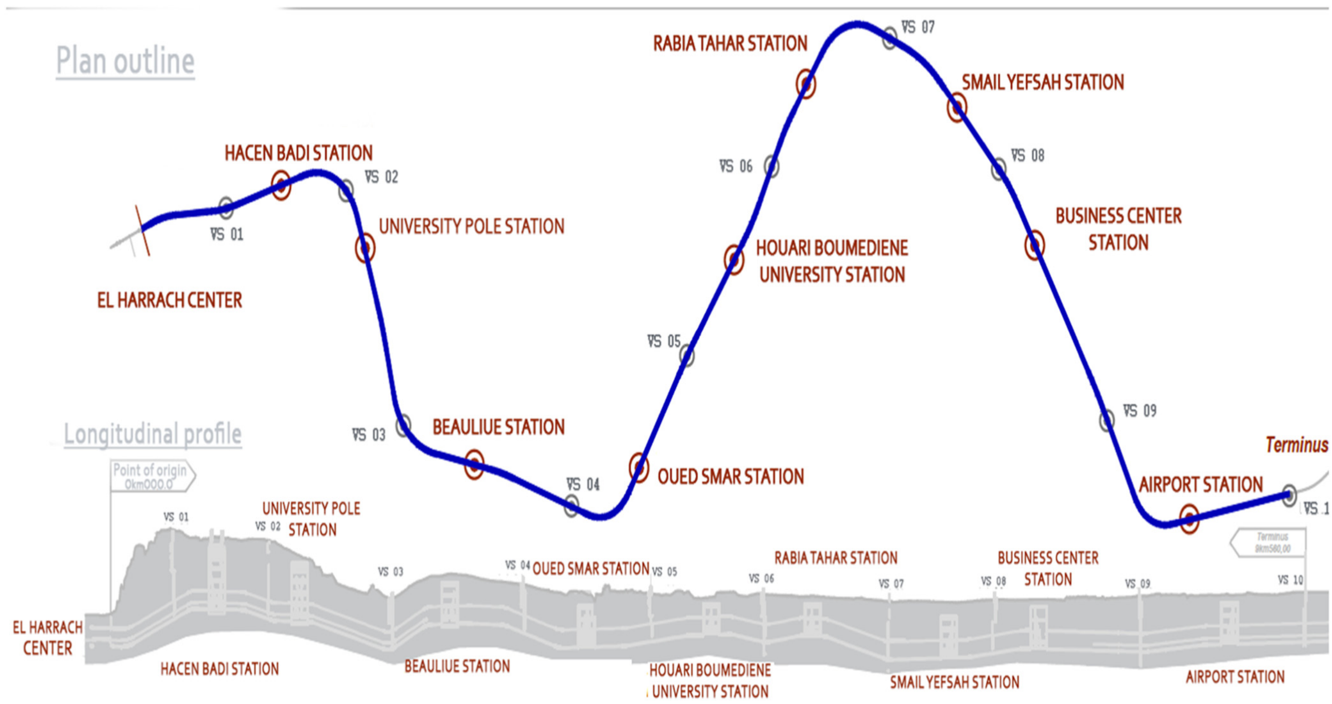

Figure 2.1. Algiers Metro line "1" extension

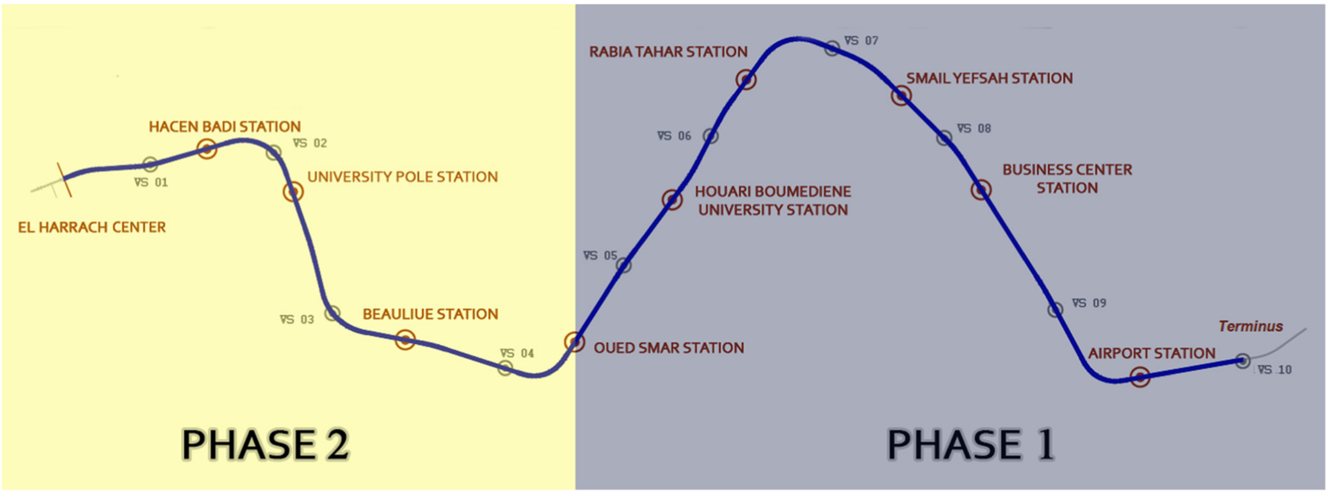

Figure 2.2. Construction phases of the tunnel project. Phases 1 and 2 correspond to zones 1 and 2, respectively, as defined in the subsequent sections

2.2. Settlement Monitoring Instruments.

The ground surface settlements were monitored using a combination of surface and subsurface instruments installed along the tunnel alignment and referenced to stable points outside the TBM influence zone.

Surface Markers and Settlement Arrays: These were installed every 12.5 to 25 m along the tunnel axis and in arrays of three markers every 50 m (one on-axis and two at ± 10 m from the axis). The markers were steel rods anchored into non-deformable structures, with daily measurements taken within a 100 m range of the TBM face.

- **Inclinometers:** Deformation within the soil was monitored using inclinometer tubes installed in boreholes with ABS pipes 55 mm in diameter. Two inclinometers were placed per

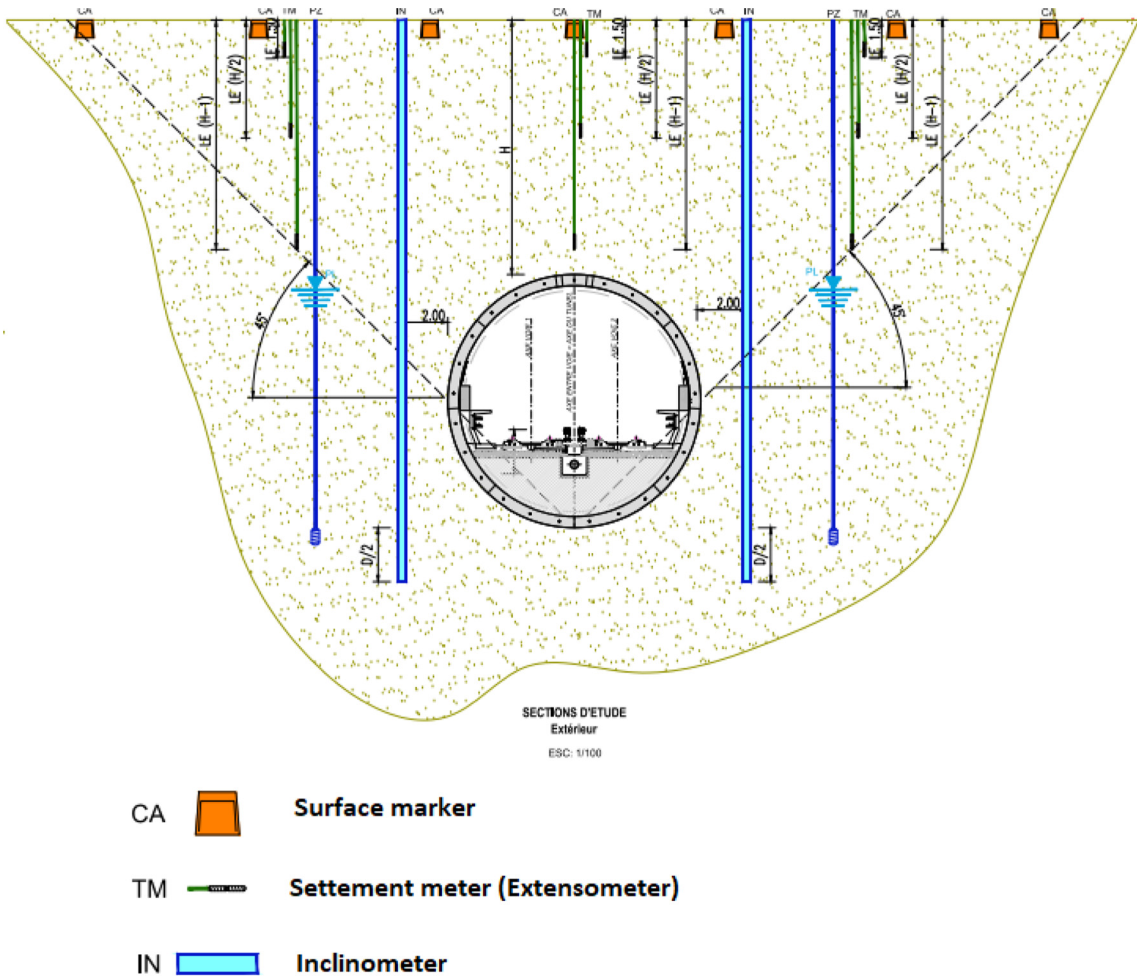

Figure 2.3. Instruments used to measure and record settlement

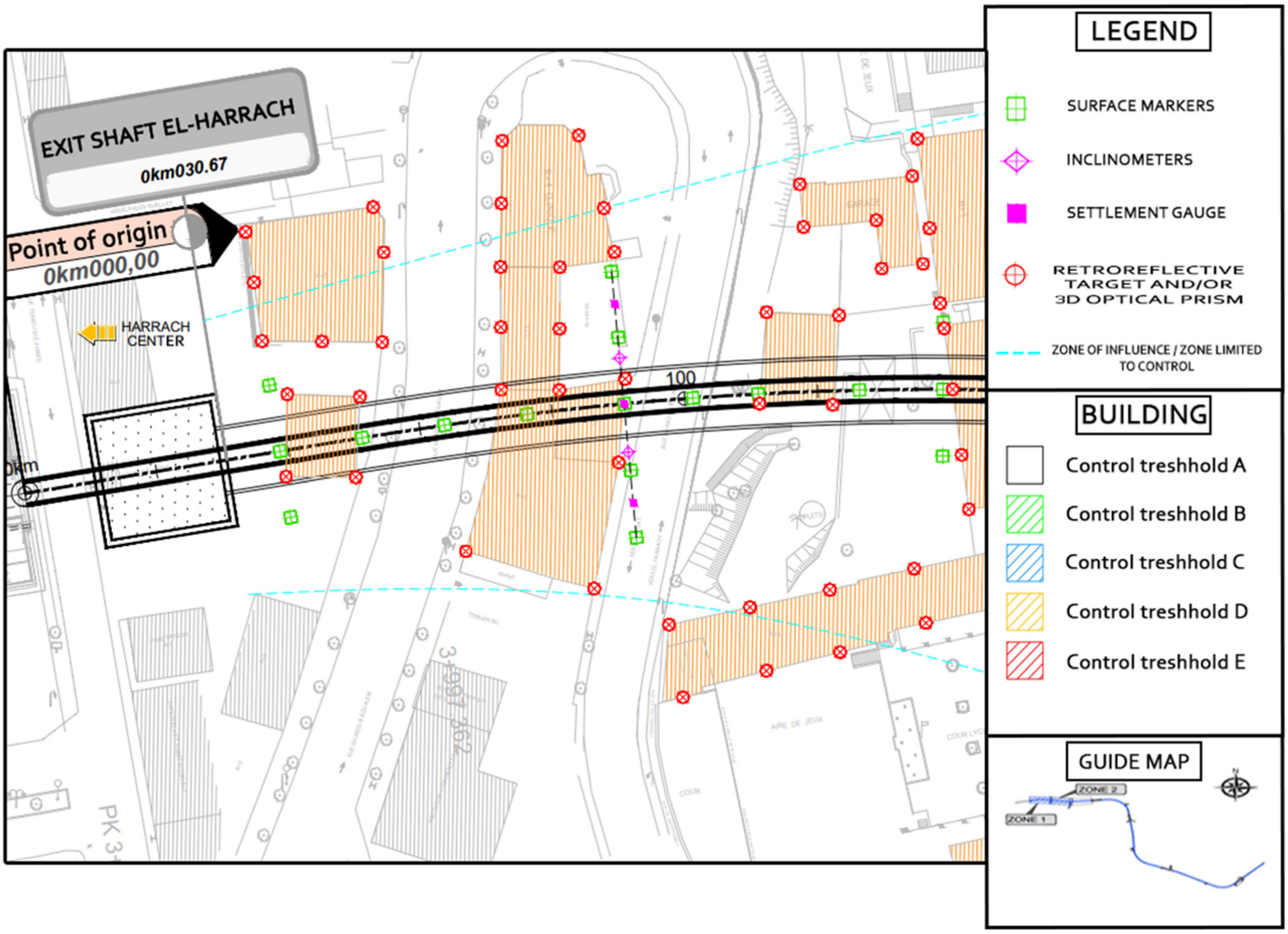

Figure 2.4. Instrument distribution plan at section pk0+000,0 to pk0+150,00

section, with readings taken after the TBM passage and when required.

- **Settlement Meters (MPBX):** These extensometers were installed at various depths in selected locations, primarily within dedicated monitoring sections. They recorded ground movements using galvanized steel rods anchored in rotary-drilled holes.

The measurement frequency varied based on TBM proximity, with high-frequency daily measurements near the face and reduced frequency once stability was confirmed. Alert thresholds were defined based on structural sensitivity (e.g., <5 mm for monumental buildings and <10 mm for surface damage-sensitive buildings).

2.3. Dataset Composition.

The ANN model was developed using a dataset of 442 samples, each corresponding to a surface monitoring point along the tunnel alignment. For each point, the associated TBM operational, geometric, and geotechnical parameters were compiled, with the target output being the maximum recorded surface settlement after the TBM passage.

2.3.1. Data Sources and Features.

This selection captures the multifactorial nature of settlement, enabling the ANN to learn from the combined physical, structural, and hydraulic influences on surface deformation.

2.4. Dataset Preprocessing.

Before model training, the dataset underwent the following pre-processing steps:

- **Cleaning:** All entries were validated for missing data, duplicates, or anomalies. Therefore, imputation was unnecessary.
- **Outlier Detection:** Visual inspection using histograms and boxplots revealed no significant outliers, warranting exclusion.
- **Normalization:** All input features were normalized using min–max scaling to the range $[-1,1]$, ensuring compatibility with activation functions and stable model convergence.

3. ARTIFICIAL NEURAL NETWORK MODELING

3.1. Background and Biological Inspiration.

ANNs are computational models inspired by the structure and function of the human brain. Each "neuron" in an ANN mimics the behavior of biological neurons by receiving inputs, processing them, and transmitting outputs to other connected neurons[13]. ANNs began as single-layer perceptrons using the delta rule and have evolved into multilayer architectures utilizing the backpropagation algorithm to adjust weights through gradient descent[14]. These models are particularly suitable for solving complex nonlinear problems, such as predicting surface settlements in tunneling operations, owing to their ability to learn intricate patterns and dependencies among input parameters.

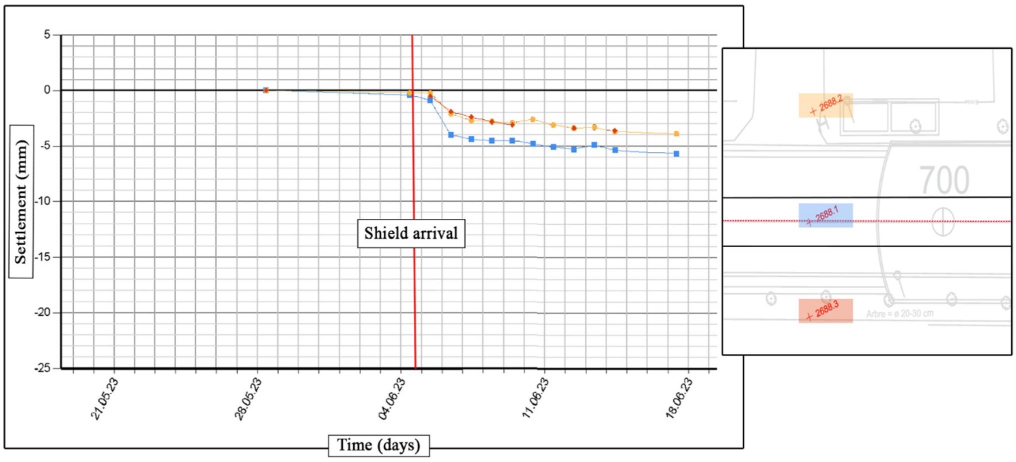

Figure 2.5. a: Recording of an array of surface markers at pk 2 +688,00

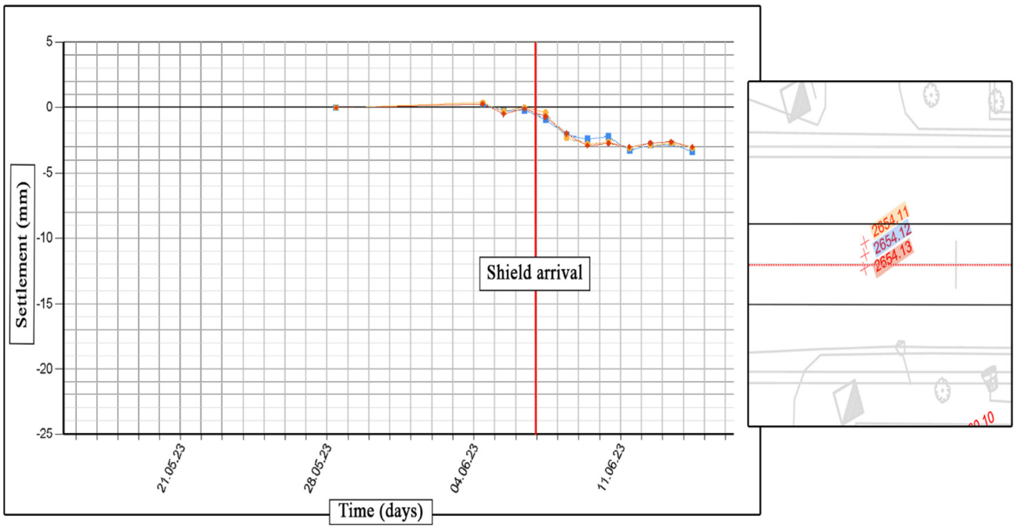

Figure 2.5. b: Settlement meter (Extensometer) recordings at pk 2 +654,00

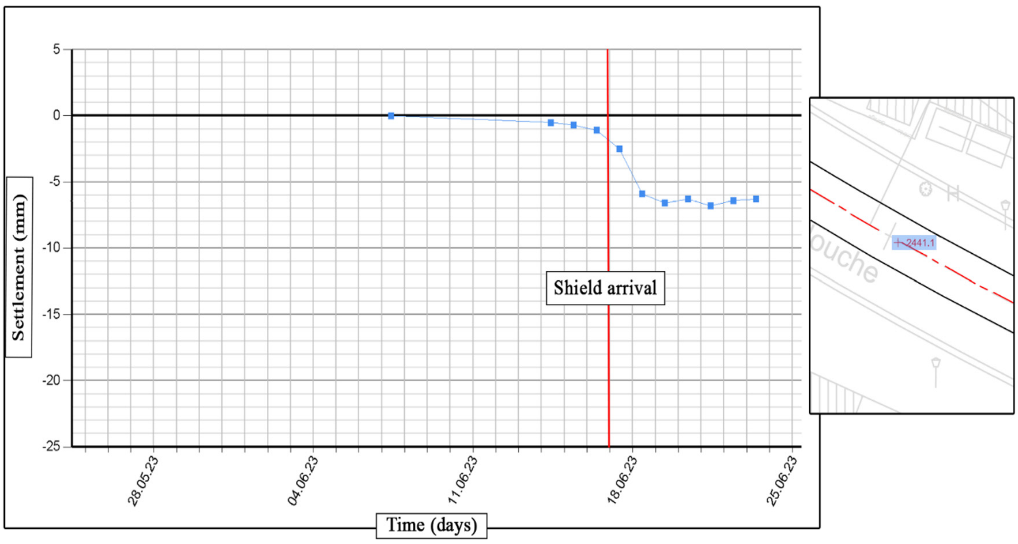

Figure 2.5. c: Recording of a surface marker at pk 2 +441,00

Table 2.1. *Summary of Features sources*

Feature	Source	Unit	Description
Penetration rate	TBM logs	mm/min	Average advance rate per ring
Face pressure	TBM logs	bar	Mean of crown sensor readings (S01, S10, S11)
Thrust	TBM mining reports	kN	Axial force applied by jacks
Grout volume	TBM mining reports	m^3	Volume of injected two-component grout
Mass loss	TBM logs	%	Mass difference relative to theoretical volume
Equivalent cover depth	Geological + geometric profile	m	Weighted soil cover depth (accounting for unit weights)
Distance from station	Tunnel layout	m	Chainage-based distance to the nearest station
Groundwater Head	Hydrogeological profile	m	Vertical difference between piezometric level and tunnel invert
Soil Deformability (EM/pl)	Pressuremeter test results	/	Ratio of Menard modulus to limit pressure, averaged by soil section

Feature	Type	Data (442 samples)				
		Minimum	Maximum	Mean	Standard Deviation	Coefficient of Variation
Penetration rate (mm/min)	Input	9.56	55,45	29,14441	8,17605	0,28054
Groundwater head (m)		0	17.3	8,32429	3,86505	0,46431
Mass loss (%)		-94.3	62,44	-1,36681	13,21872	9,67122
Thrust (KN)		12833,69	86378,78	33408,00835	11854,12791	0,35483
Equivalent CD (m)		9,48	40,65	18,46077	5,93975	0,32175
Face pressure (bar)		0,39	2,7	1,25052	0,45359	0,36272
Grout volume (m^3)		3	11,36	8,58183	1,18081	0,13759
Distance from Station (m)		5	1343	454,45226	291,2336	0,64085
$\frac{E_M}{Pl}$		4.23	53.76	19,29792	8,42018	0,43633
Settlement (mm)	Target	-80	0	-7,03767	9,82042	1,39541

Figure 2.6. Summary of descriptive statistics of considered features

3.2. Design of the Optimal Neural Network.

Determining the optimal network architecture, particularly the number of neurons in the hidden layers, is a crucial step in the modeling process. This aspect has been extensively studied in feedforward backpropagation neural networks, and two principal methodological strategies have emerged: constructive approaches [15] and pruning strategies [16]. In this study, a constructive approach was adopted using a trial-and-error method, in which various configurations of hidden neurons were tested iteratively by incrementally adding neurons to the hidden layer. Each configuration was trained using a predefined data division, and its performance was evaluated using two key statistical indicators: RMSE and R^2. Determine which network structure best balances the accuracy and model simplicity.

3.3. Implementation.

3.3.1. Computational Environment. MATLAB was employed as the main computational platform for developing, training, and simulating the ANN model, primarily because of its dedicated Neural Network Toolbox and optimized training

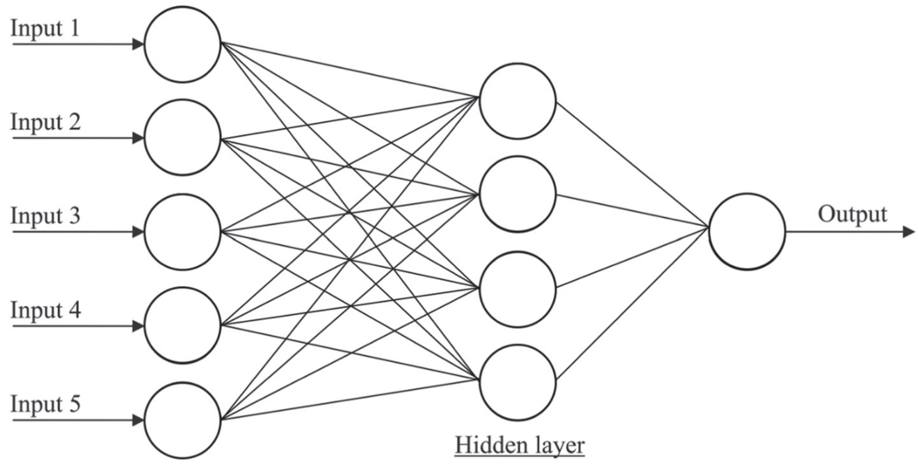

Figure 3.1. Multi-layer ANN

functions. Python was used extensively during the preprocessing and exploratory phases, particularly for data cleaning, normalization, and visualization. The final model development and sensitivity analyses were conducted using the MATLAB software. As a starting point, we utilized the FitNet configuration provided by the MATLAB neural network Fitting Tool, which is specifically designed for functional approximation problems using feedforward neural networks. The default configuration of Fitnet includes the following key characteristics:

Table 3.1. *Default fitnet Configuration in MATLAB*

Neural network model	Feedforward backpropagation Neural network
Hidden layer	Single hidden layer
Training network algorithm	Levenberg-Marquardt
Transfer function hidden layer	`tansig`
Transfer function output layer	`purelin`
No. of epochs	1000
Validation checks (iterations)	6
Performance	MSE and R2

3.3.2. Neural Network Training Procedure.

To develop an effective neural network model for predicting ground surface settlement, a full-scale training phase was conducted using the entire dataset with appropriate data partitioning to ensure a robust model evaluation. The dataset was divided into three subsets: 70% training (310 samples), 15% validation (66 samples), and 15% testing (66 samples). This approach enables both model learning and independent performance assessment while preventing data leakage. A Feedforward Backpropagation Neural Network (FF-BP-ANN) was employed with an input layer consisting of nine neurons corresponding to the nine selected input features (Fig. 3.3). Various hidden layer configurations were systematically tested to identify the network architecture that provided the best generalization performance. Once the optimal configuration was identified, it was evaluated on the test set to assess its predictive capability for unseen data.

4. MODEL PERFORMANCE, COMPARISON WITH ALTERNATIVE METHODS, AND SENSITIVITY ANALYSIS

4.1. Model Performance ANN.

Sixteen configurations with different numbers of neurons in each hidden layer were tested. For each configuration, the network was trained 15 times, allowing for slight variations owing to random initialization and data shuffling. From these repetitions, the best-performing result, based on the highest validation and test R^2 value, was retained to represent each configuration. This repetitive training ensured that the evaluation of each architecture was not biased by outliers or unstable initial conditions and that the peak performance for each structure was reliably captured. The results shown in Fig. 3.4 present R^2 for the training, validation, testing, and overall data across all configurations. The graph clearly shows that the performance initially improved as the number of neurons increased. The optimal performance was achieved with eight neurons, where the model attained R^2 values close to 0.94 for all three phases.

Beyond 10 neurons, although the training R^2r remained high or increased, suggesting a tighter fit to the training data, the

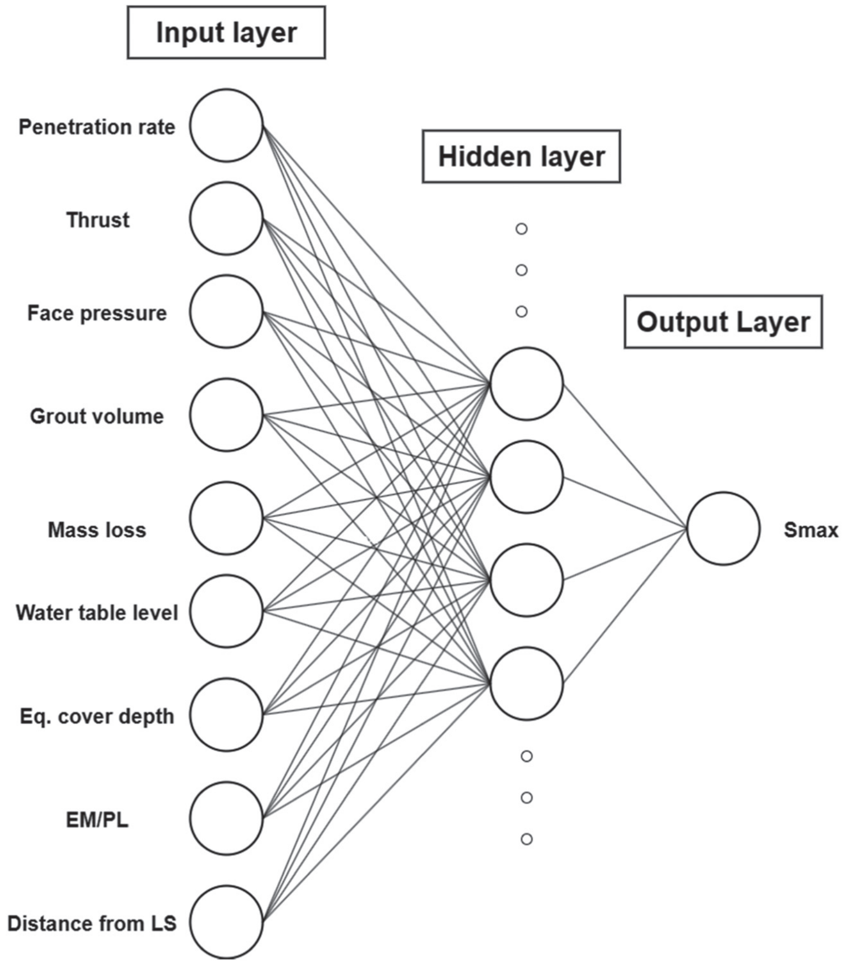

Figure 3.2. Neural Network Input Configuration

validation and test R^2 values began to decrease in several configurations. This divergence reflects signs of overfitting, where the model becomes too specialized for the training data and loses its ability to generalize. Another evaluation step in the pre-assessment of networks is illustrated in Fig. 3.5, which presents the RMSE values of all the generated networks on the test

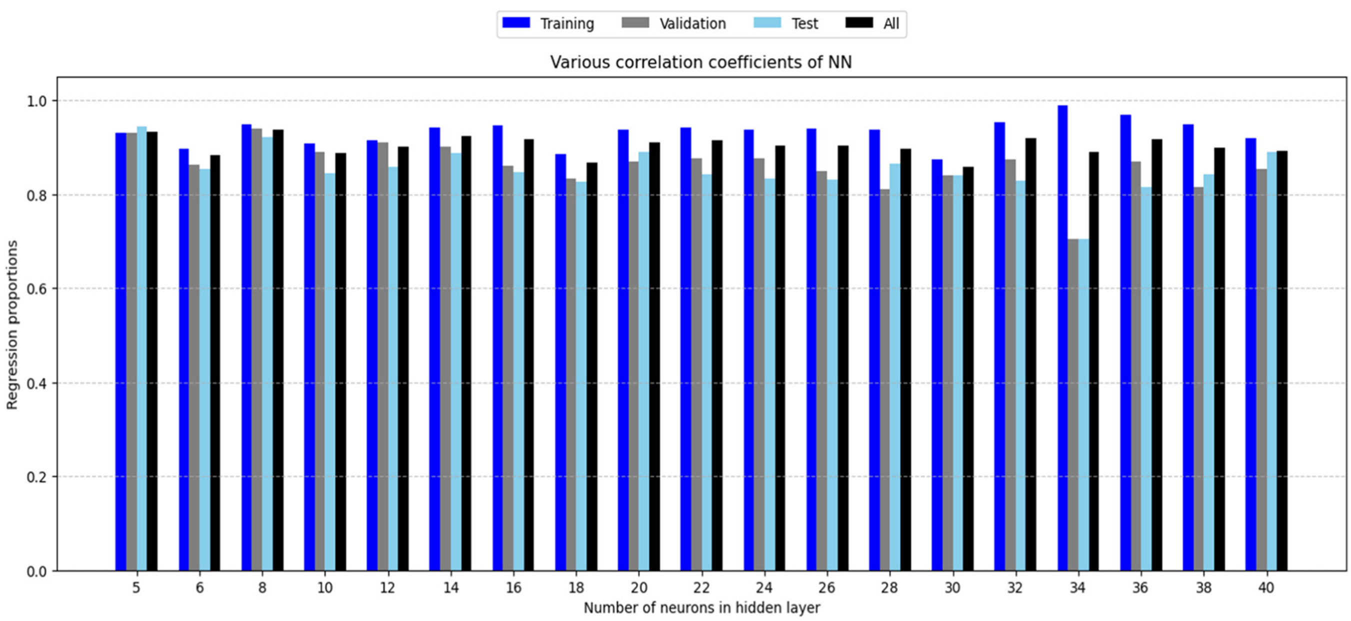

Figure 4.1. R^2 across Neuron Configurations

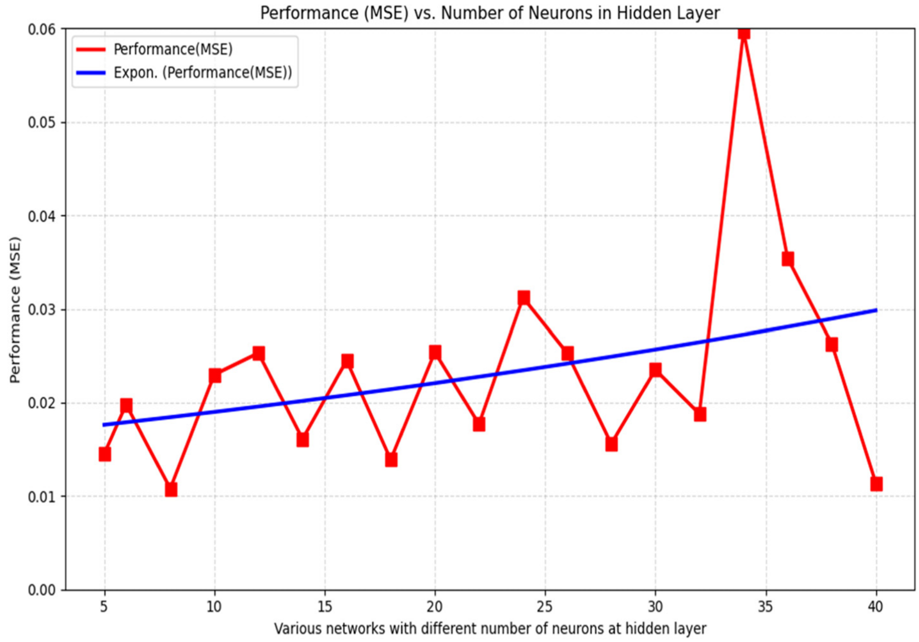

Figure 4.2. RMSE for Different NN in Hidden Layer

dataset. The 9-8-1 architecture achieved the lowest RMSE of 4.16 mm, indicating a strong performance. In contrast, the 9-34-1 network exhibited the highest RMSE of 9.77 mm. The curve labeled Expon (Performance (RMSE)) represents an exponential fit applied to the data to model the overall trend of the RMSE evolution as the number of neurons in the hidden layer increases.

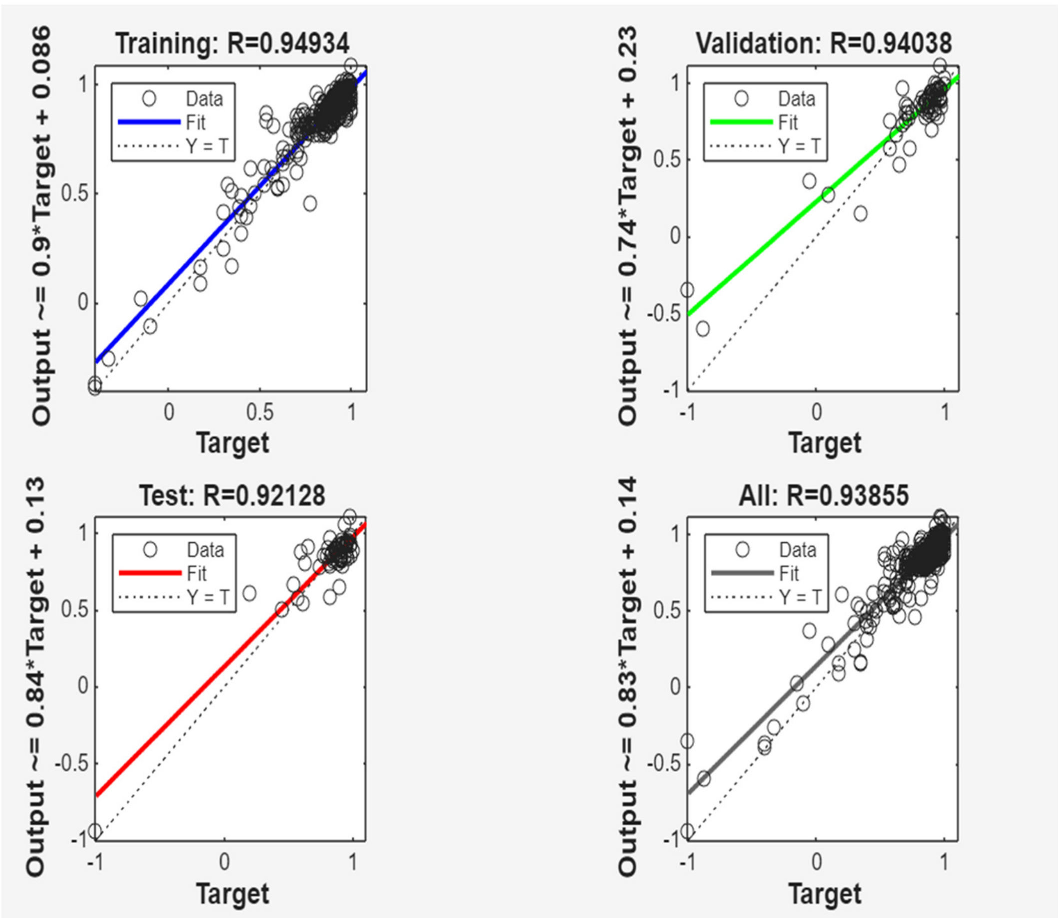

Figure 4.3. Regression Plots for Training, Validation, Testing, and Overall

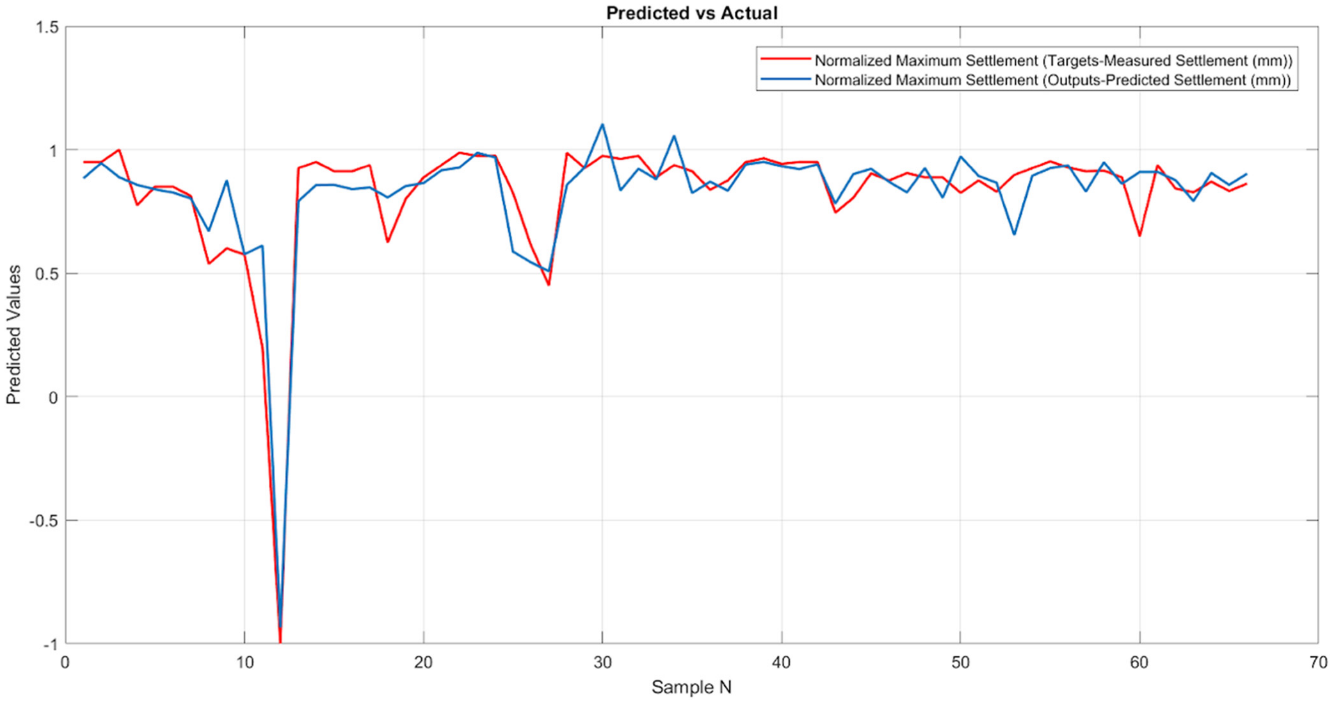

Figure 4.4. Predicted Settlement vs Actual Settlement for the Test Dataset

4.1.1. Prediction of Maximum Settlement Using the Most Accurate Neural Network. In this study, several neural network architectures were designed and evaluated to predict the surface settlement induced by excavation using EPB-TBM. After a series of tests, the NN 9-8-1 model was identified as the most effective because of its high accuracy and stability throughout the different training phases.

The results obtained, presented in Fig. 4.3, show very good agreement between the predicted values and the measured settlements, with correlation coefficients of R^2 =0.949 for training, $R^2 = 0.94$ for validation, and $R^2 = 0.92$ for testing, all exceeding 0.90. Fig. 4.4 presents a comparison between the normalized measured settlements (in red) and normalized predicted settlements (in blue) for the Test Dataset. The close agreement between the two curves across most of the test sample ranges reflects the ability of the model to accurately reproduce the overall settlement trend.

Fig. 4.5 displays the residual error plot, which illustrates the difference between the measured and predicted settlement values across all monitoring points along the tunnel alignment. Each blue dot represents the residual error at a given location, and the red line indicates the zero-error reference. The residuals appear to be symmetrically distributed around zero.

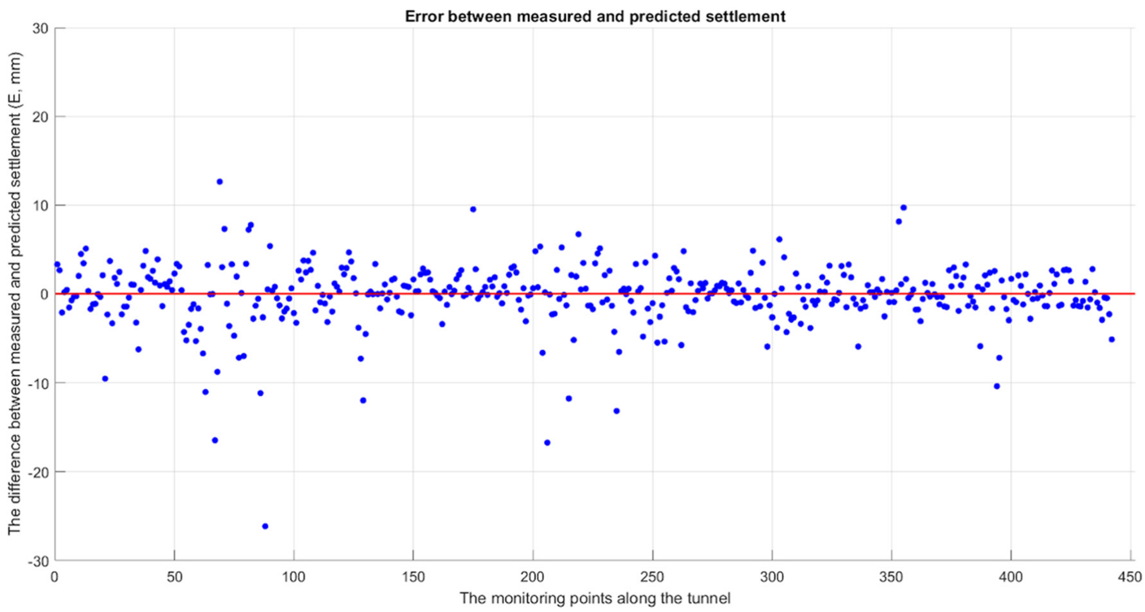

Figure 4.5. Residual Error Distribution of Predicted vs Measured Settlements along the Tunnel Alignment

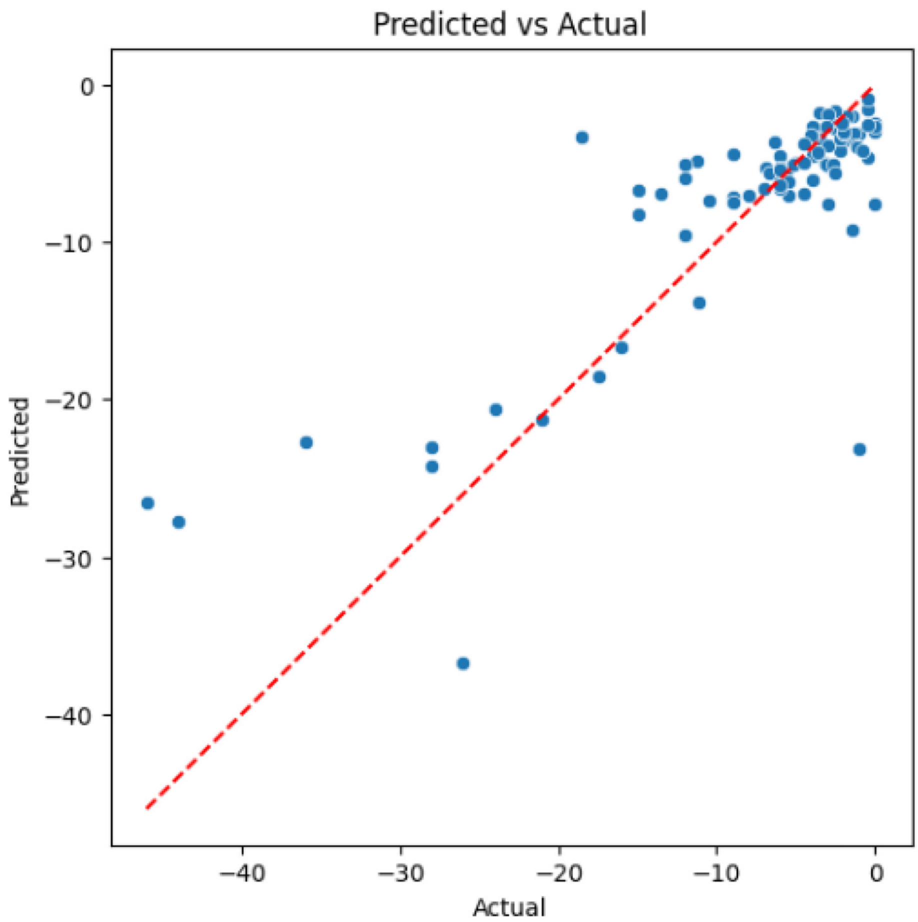

Figure 4.6. Regression plot for RF

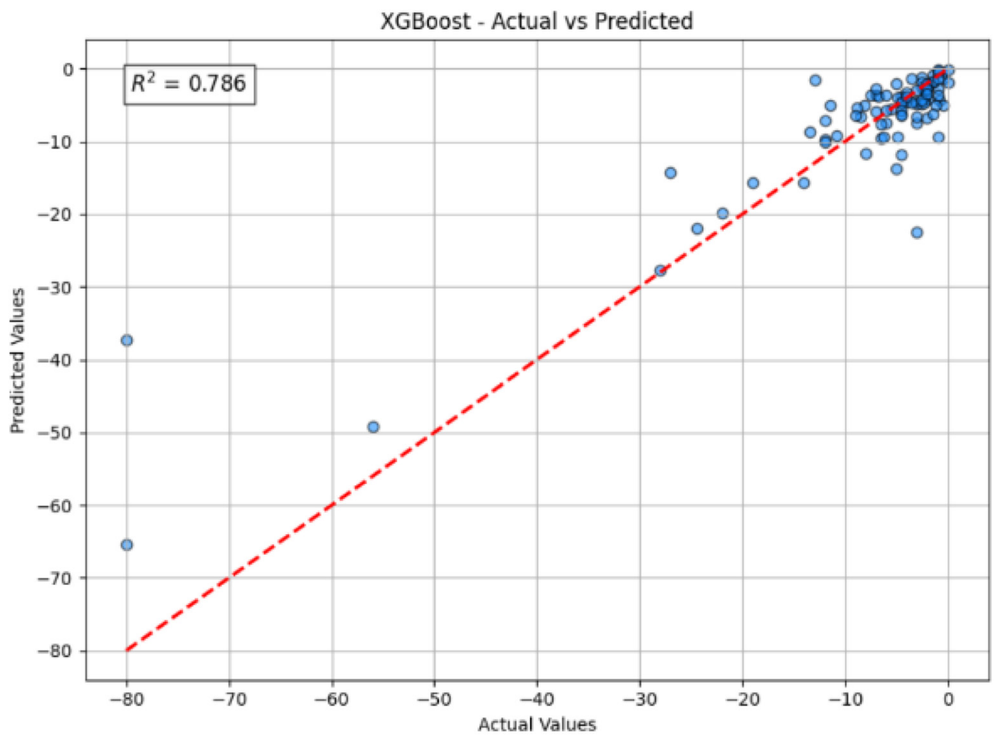

Figure 4.7. Regression plot for XGBoost

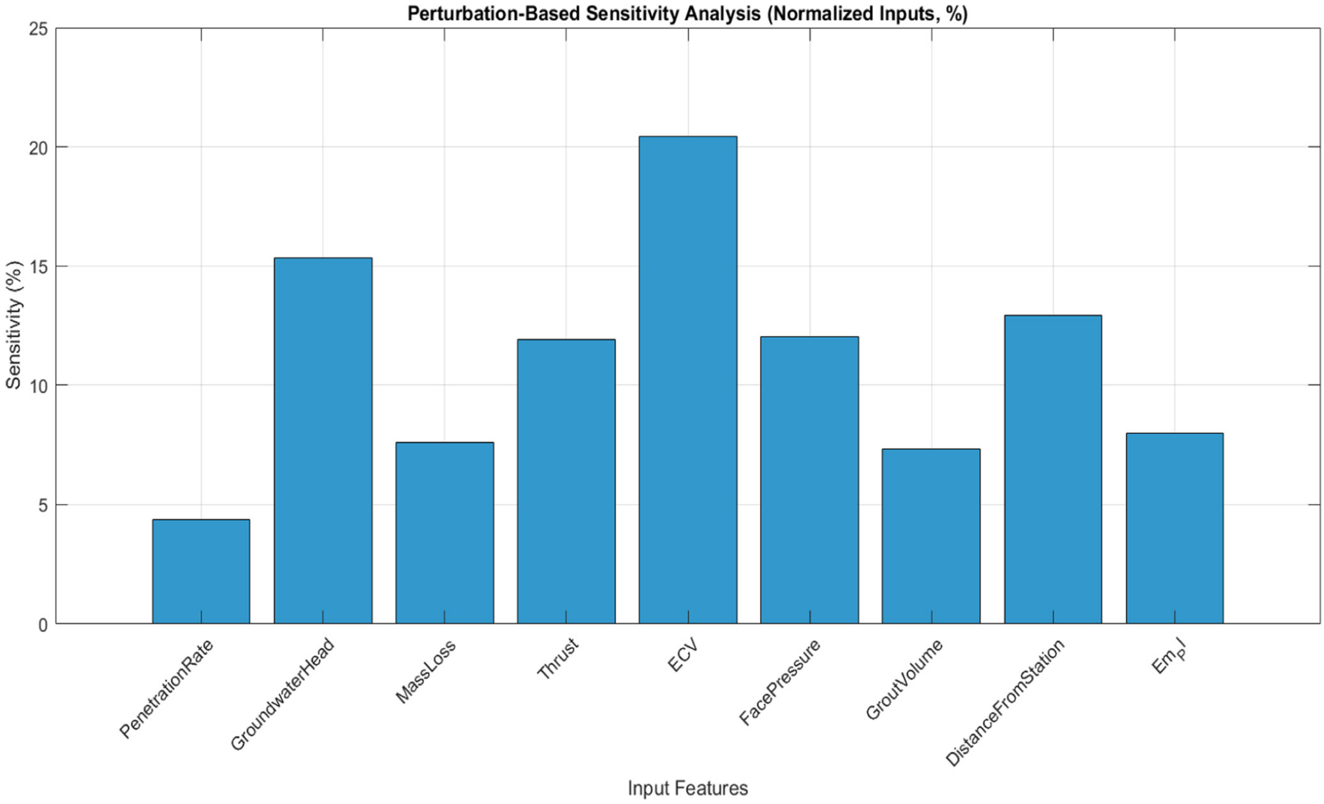

Figure 4.8. Perturbation-based sensitivity analysis with 10% input variation

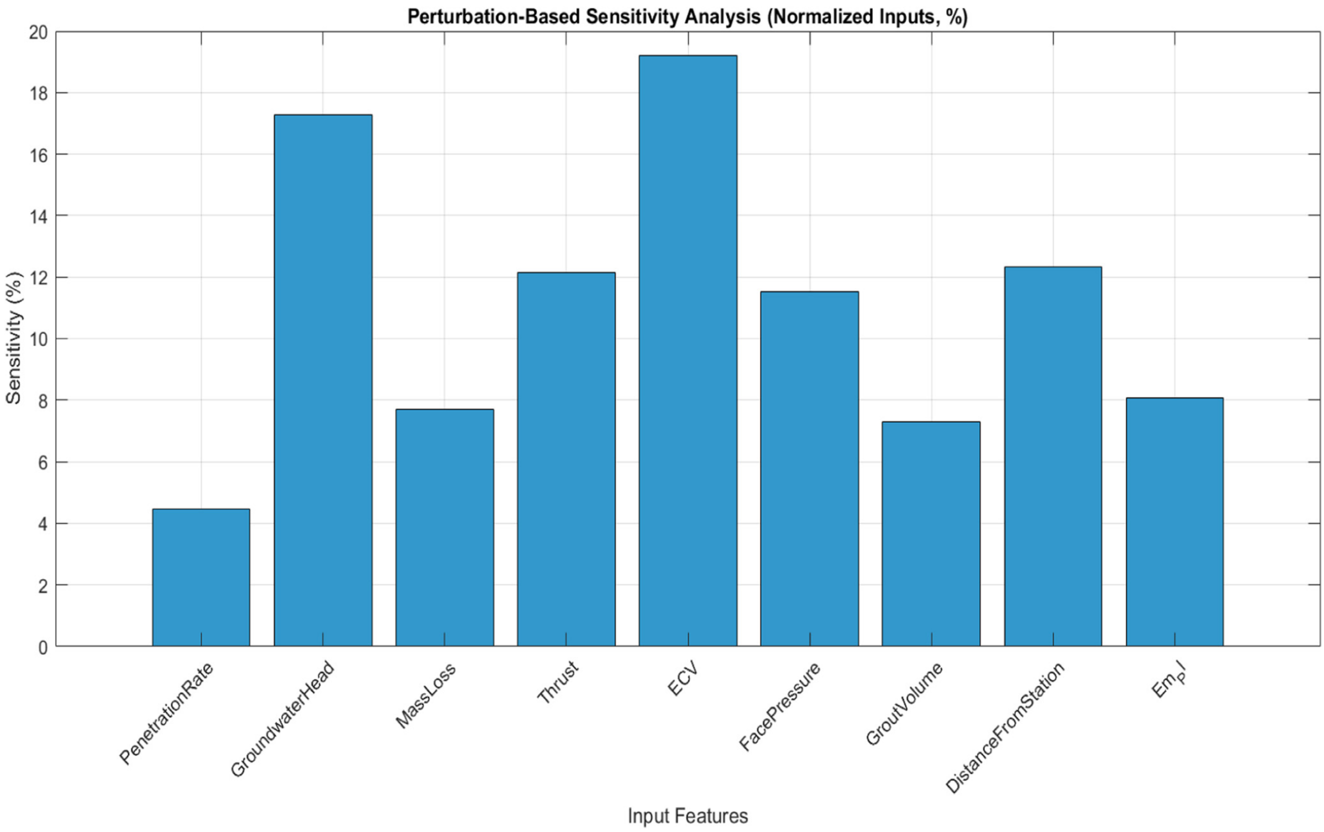

Figure 4.9. Perturbation-based sensitivity analysis with 15% input variation

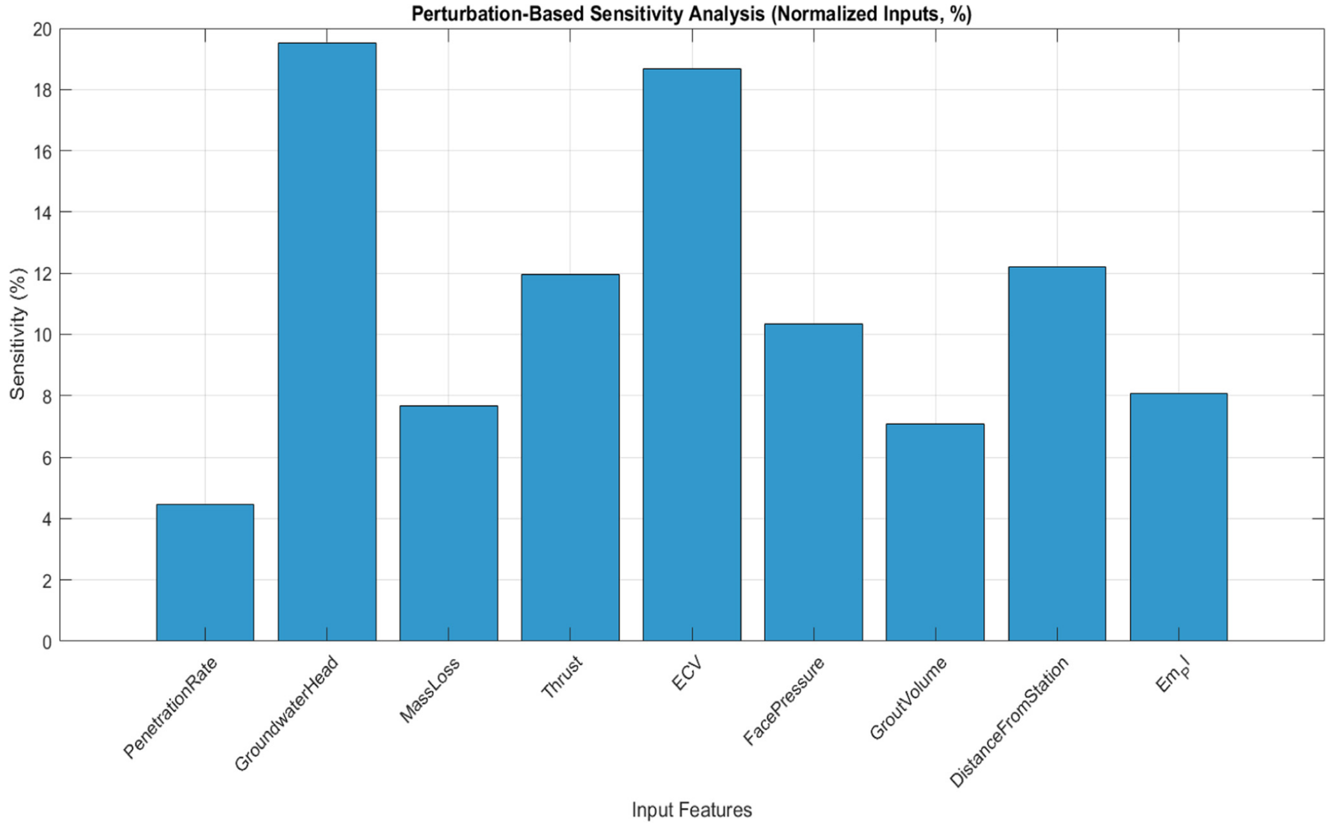

Figure 4.10. Perturbation-based sensitivity analysis with 20% input variation

4.2. Comparison with Tree-Based Machine Learning Models. To evaluate the robustness and generalizability of the ANN approach, its performance was compared with two widely used tree-based models: Random Forest and Extreme Gradient Boosting (XGBoost).

4.2.1. Random Forest . With zero-controllable hyperparameters, the model can be applied to both regression and classification tasks. The following results were obtained:

R^2 Score:	0.679
RMSE (mm):	5.09

4.2.2. Extreme gradient boosting . These results were obtained using the following hyperparameters.

Learning rate	0.2
Maximum depth of each tree	5
Fraction of the data to be randomly sampled for growing each tree	1
Fraction of features used to build each tree	0.8

R^2 Score:	0.7859
RMSE (mm):	6.17

These comparisons emphasize the strength of the ANN in capturing the nonlinear and multidimensional interactions inherent to tunneling-induced settlement processes. Unlike tree-based models, ANNs do not rely on the implicit assumptions of hierarchical feature splitting, which allows them to model continuous and interdependent variables more accurately

4.3. Sensitivity Analysis. After evaluating the performance of the selected neural network architecture (9-8-1) on the test dataset and confirming its high predictive accuracy and low error metrics, conducting a sensitivity analysis was appropriate.

4.3.1. Perturbation Sensitivity Analysis. The figures present the results of the perturbation-based sensitivity analysis performed on the test dataset. Three perturbation magnitudes 10%, 15%, and 20% were applied systematically to each input feature. The corresponding changes in the predicted maximum surface settlement were recorded to evaluate the relative sensitivity of the model for each parameter.

4.3.1.1 Results Analysis. The results obtained for the three levels of perturbation show that for the first two successive values of $\pm10\%$ and $\pm15\%$, the three most influential parameters on the prediction results are equivalent cover depth, groundwater head, and distance from the station. However, for $\pm20\%$ variation, a change was observed in the ranking of the three most influential parameters. This suggests that the model exhibits strong nonlinear behavior or instability when the perturbation amplitude becomes significant.

In the present case, the decision to retain the results obtained with a $\pm15\%$ perturbation was made for two main reasons:

- This reflects a realistic range of variability in geotechnical and operational parameters, ensuring that the analysis remains relevant to practical engineering conditions.

Table 4.1. *Synaptic Weights Connecting the Input, Hidden, and Output Layers of the Trained ANN*

	Inputs									Target
	TBM params					Geology		Geotechnical parameters	Geometry	Settlement
	Penetration rate	Thrust	Face pressure	Grout volume	Mass loss	Ground water head	Equivalent Cover depth	EM/PL	Distance from Station	
Hidden neurons	Penrate variable weights	TH variable weights	FP variable weights	GV variable weights	ML variable weights	WTL variable weights	ECD variable weights	EM/PL variable weights	DS variable weights	Smax variable weights
1	0.12914	-0.38366	1.16181	-0.03607	1.22441	6.54519	-4.39802	0.17999	3.78295	-3.95595
2	0.75635	0.63084	-1.59512	-0.31161	-0.18384	-0.08581	-2.11306	-1.01983	0.98319	-2.31137
3	-0.91774	-0.98713	2.85070	0.42518	0.04268	-0.00837	3.87149	0.86859	-1.34541	-1.74814
4	0.04452	-0.42354	-0.48498	-0.06413	-1.07588	-6.41319	4.94460	-0.04235	-3.32660	-3.92278
5	0.04578	0.65607	0.33131	-2.60266	-1.68915	1.36805	2.06010	-0.84492	-0.13516	0.38029
6	-0.40639	0.66091	0.45652	-3.38484	3.08497	2.54837	0.12188	2.82609	-3.41657	0.17907
7	-0.06273	-0.41411	-0.49601	2.06026	0.69205	-1.11673	-1.65835	-0.05515	0.73264	0.56747
8	0.43403	0.01190	-5.14714	0.66119	0.12270	0.79422	-8.26129	1.57529	0.63891	-0.58807

- This is sufficiently pronounced to capture potential nonlinear interactions within the model without introducing excessive distortions in the output.

4.3.2. Weight-based Sensitivity Analysis. The analysis was conducted by extracting and evaluating the synaptic weights connecting the input, hidden, and output layers, as listed in Table 4.1.

The necessary computations were performed to calculate the Individual Input Factor IIFi for each input parameter using the

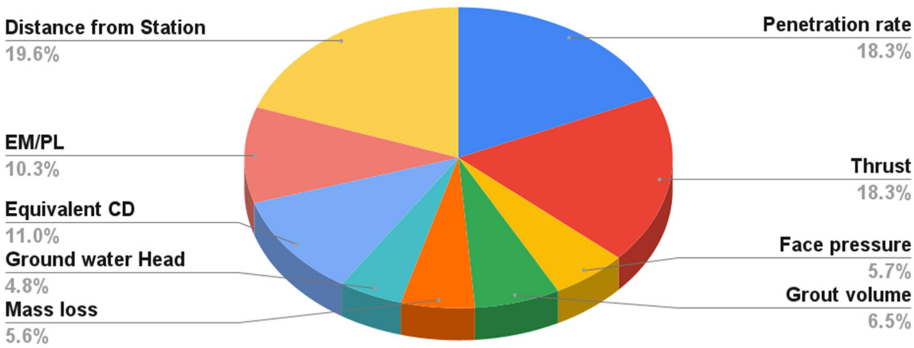

Figure 4.11. Weight-based Sensitivity Analysis result

Table 5.1. *Results of the perturbation-based sensitivity analysis*

Input Parameter	Relative Influence (%)
Equivalent Cover Depth (ECV)	19.1
Groundwater Head (Water Table Level)	17.3
Distance from Station (DistS)	12.2
Thrust	12.2
Face Pressure	11.5
E_M/p_l	8.3
Mass Loss	7.6
Grouting Volume	7.2
Penetration Rate	4.7

Milne method (Equation 1):

$$IIF_i = \frac{\sum_{j=1}^{n} |w_{ij}|}{\sum_{i=1}^{m}\sum_{j=1}^{n} |w_{ij}|} \tag{1}$$

Where:

- w_{ij} = Weight between input neuron I and hidden neuron j
- m = Total number of input neurons
- n = Total number of hidden neurons
- $|w_{ij}|$ = Absolute value of the weight

The resulting sensitivity values are presented in Fig. 4.11.

5. DISCUSSION

Following the application of both perturbation- and weight-based (Milne) sensitivity analyses, several important insights emerged regarding the influence of each input parameter on the predicted ground surface settlement. Although both approaches aim to assess the variable importance, they provide distinct yet complementary insights, revealing both converging and differing patterns that enhance the interpretation of an ANN's internal logic and its representation of the underlying physical phenomena.

The perturbation-based analysis, which quantified the effect of ±15% variations in each input on the output of the model, identified the most sensitive parameters, as listed in Table 5.1.

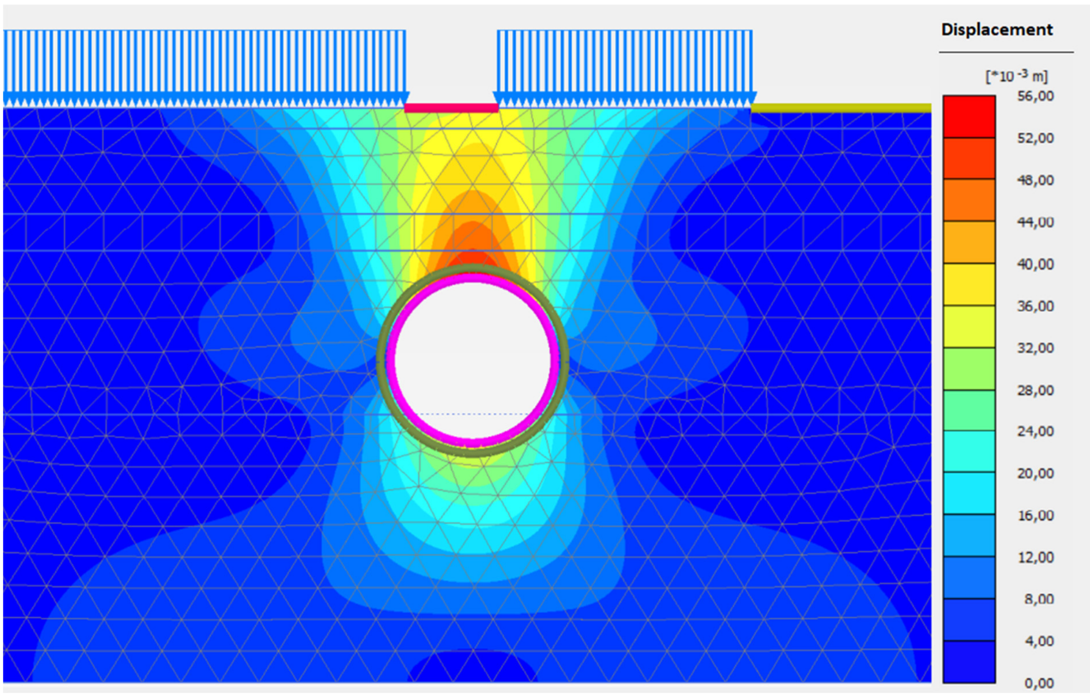

Figure 5.1. Simulation under Plaxis 2D software showing the arching zone for a tunnel depth of 20m (Extension line 1)

These findings underscore the strong influence of geometric and hydrogeological conditions on the ground surface settlement. This aligns with the fundamental geomechanical principles: a greater overburden increases the vertical stress at the tunnel vault depth, amplifying the potential for downward soil movement toward the tunnel face. If this displacement is not properly controlled, it can propagate upward and manifest as surface settlement. However, the ability of the ground to resist such deformation is strongly linked to the cover depth through the arching effect, whereby a greater depth provides sufficient confinement for the soil to laterally redirect vertical stresses around the tunnel, limiting deformation above the crown and reducing surface settlement. This phenomenon is illustrated in Figs. 5.1 and 5.2.

This indicates significantly lower displacement values above the tunnel crown as the cover depth increased. Conversely, the Algiers Metro tunnel, characterized by predominantly shallow equivalent cover depths (13–25 m), demonstrates an insignificant arching effect, resulting in greater vulnerability to surface settlement. As depicted in Fig. 5.1 for a 20m cover depth, the displacement becomes notably more pronounced above the tunnel crown at shallow depths. Similarly, elevated groundwater levels reduce the effective stress and may lead to soil softening and increased susceptibility to deformation. Prior research on tunneling through water-rich or soft soils supports this, often showing a near-linear relationship between groundwater fluctuations and the magnitude of the surface settlement.

In contrast, Milne's weight-based analysis, which evaluates the contribution of each input based on the magnitude of the normalized weight paths within the network, placed a greater emphasis on parameters associated with machine operation, such as thrust and penetration rate. This suggests that, during training, the network structurally relied on these variables, even if the predicted output did not strongly react to small perturbations in their values. A particularly noteworthy outcome was the consistent prominence of Distance from Station in both analyses. This parameter likely captures a positional or temporal trend: sections closer to stations are encountered during the early tunneling stages when the TBM may not yet be fully stabilized. In these zones, machine parameters, such as thrust and penetration rate, may exhibit greater variability, increasing the likelihood of surface disturbance. The ANN appears to have learned this implicit condition, associating early-stage tunneling operations with an increased settlement risk. Thrust and face pressure emerged as key operational parameters influencing surface settlement, each playing a distinct but interconnected role in TBM performance. The thrust directly governs the forward advance of the machine and contributes significantly to face stability. Sensitivity analysis confirmed its strong influence, with high scores in both the perturbation- and weight-based methods. The face pressure, while showing only moderate sensitivity (5.7% structural importance), is critical for counteracting earth and water pressures at the tunnel face, particularly in weak soils or under high groundwater conditions. These two parameters were highly interdependent. An increase in thrust, if not balanced by an adequate face pressure, can destabilize the face and induce excessive ground deformation. Conversely, excessive face pressure with insufficient thrust can reduce the advance efficiency or cause blowouts. The ANN likely captured this dynamic, assigning importance to both features while moderating their standalone sensitivity based on how they varied together in the dataset.

The penetration rate further reinforces this interdependence. Although it received the second-highest structural importance in the Milne weight-based analysis (18.3%), it showed the lowest perturbation sensitivity. This discrepancy suggests that the influence of the penetration rate is conditional, meaning that it only significantly affects the settlement when combined with specific thrust and face pressure conditions. This is supported by its

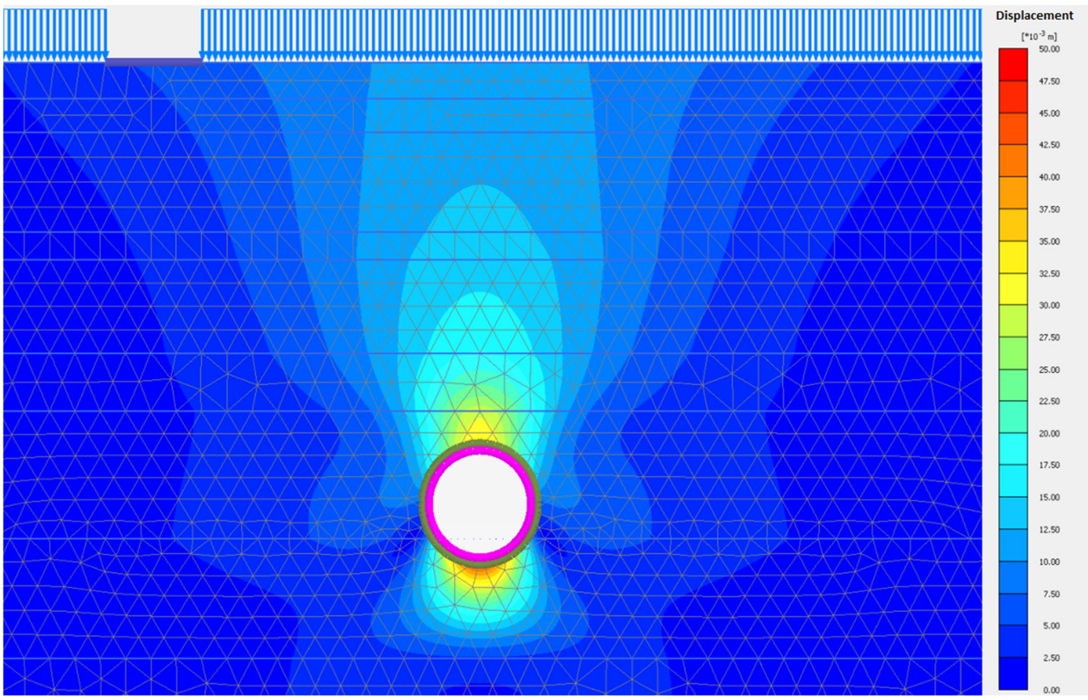

Figure 5.2. Simulation under Plaxis 2D software showing the arching zone for a tunnel depth of 66m (Extension line 1)

statistical distribution: being approximately normal and centered at approximately 30 mm/min, small perturbations often remain within operationally stable limits. Therefore, the penetration rate alone may not trigger large prediction changes; however, it acts as an informative indicator of how thrust and face pressure interact, reflecting the efficiency of TBM advancement and stress transmission to the ground. The EM/pl ratio showed a measurable and consistent influence on the predicted settlement, indicating that the ANN captured the link between the soil deformability and ground response. Lower values, reflecting more compressible soils, are associated with increased settlement under TBM-induced loading.

The grouting volume and mass loss exhibited low but non-negligible importance in both analyses. Although consistently ranked near the bottom, the perturbation results showed that they could influence settlement predictions under specific conditions. Their limited but measurable effects suggest that although they are not primary drivers, they may contribute to context-dependent scenarios.

6. CONCLUSIONS

This study successfully developed an ANN model to predict the maximum ground surface settlement induced by EPB-TBM tunneling in the Algiers Metro project. This study integrated machine learning with geotechnical engineering, yielding a robust predictive tool while providing interpretable insights into the key factors influencing settlement.

Key Findings

- **Optimal ANN Architecture**
- A feedforward backpropagation ANN (9-8-1) with eight hidden neurons achieved the best performance, yielding R^2 values above 0.92 across all datasets and maintaining a low prediction error with an RMSE of 4.16 mm.
- The Levenberg–Marquardt optimization algorithm and tanh/purelin activation functions proved effective in modeling the nonlinear relationships between TBM operations and settlement.
- The ANN outperformed traditional machine-learning models, namely Random Forest and XGBoost, in terms of prediction accuracy and generalization. The tree-based models showed lower R^2 values (0.679 and 0.7859, respectively) and higher RMSEs, indicating their limitations in modeling settlement patterns in geotechnically variable contexts.
- **Sensitivity Analysis Insights**
- Perturbation-based analysis (±15% variation) revealed that Equivalent Cover Depth (ECV) and Groundwater Head were the most influential factors, followed by Distance from Station (DistS) and Thrust/Face Pressures.
- Weight-based analysis (Milne method) highlighted the Thrust and Penetration Rate as structurally significant despite their lower perturbation sensitivity.
- The differences between the analysis methods reveal that parameters such as the Penetration Rate, which are structurally important to the ANN, exert their influence primarily through interactions with other key variables rather than in isolation.
- **Geotechnical and Operational Implications**
- A Shallow Equivalent Cover Depth (ECV) and elevated groundwater levels were identified as key contributors to surface settlement. A reduced cover depth diminishes the arching effect that normally shields the ground surface, whereas high groundwater lowers the effective stress and softens the soil, increasing the susceptibility to deformation during excavation.
- Early-stage tunneling at a low Distance from Station was associated with an increased settlement risk, likely due to transitional TBM behavior before reaching operational stability.
- Penetration Rate serves as an indirect indicator of TBM–ground interaction dynamics. Although relatively insensitive to small input variations, it reflects the coordinated effect of thrust and face pressure, making it a valuable parameter for assessing excavation efficiency across varying ground conditions.
- Grouting Volume demonstrated low sensitivity across both analytical methods, suggesting a minor overall role in predicting settlement. However, its consistent presence indicates a potential influence in specific contexts, particularly where proper compensation of the annular void is essential to maintain ground stability, such as in loose or low-cohesion soils. In such cases, inadequate grouting may allow void migration or relaxation, which subtly contributes to deformation.
- Mass Loss also showed a consistently low sensitivity across both methods, reinforcing its limited general impact on settlement prediction. Nevertheless, under certain conditions, such as weak confinement or face instability, they may indirectly contribute to ground deformation. These scenarios often involve over-excavation or insufficient face pressure control, and even small mass losses can lead to stress redistribution and local soil loosening.
- **Practical Recommendations**

Design Phase

- An adequate cover depth should be prioritized during route selection and profile optimization. Where shallow cover cannot be avoided, mitigation should focus first on adjusting the TBM operating parameters, such as optimizing the face pressure and regulating the advance rate to maintain face stability, with targeted ground treatment or localized support measures reserved only for critical locations.
- In sections with elevated groundwater levels, pre-excavation dewatering systems (e.g., deep wells and vacuum wells) should be employed to maintain the ground strength.
- Pre-excavation ground treatments such as jet grouting should be considered near stations or when launching shafts to improve the initial TBM face stability and minimize early-stage ground deformation.

Construction Phase

- The key TBM operational parameters, particularly those that strongly interact with critical soil conditions along the tunnel alignment, should be closely monitored and controlled.
- Conduct ground response monitoring (e.g., using extensometers and settlement markers) above critical structures to detect surface movement early and allow for intervention.

Model Deployment

- Translate the model predictions into recommended adjustments that can be presented to operators in real time.
- Integrate real-time sensor data to refine predictions dynamically.
- Deploy warning thresholds in the model output to alert operators of potentially unsafe trends in settlement behavior.

Constraints and Future Work

Certain constraints on data availability and quality must be addressed during database construction and preprocessing.

- Geomechanical Parameters

Classical soil parameters such as cohesion and friction angle were not available because they were either untested or likely derived through empirical correlations rather than direct measurements. To maintain consistency with the field-based input data, the model uses the EM/pl ratio obtained from the pressuremeter tests as a proxy for soil deformability.

- Operational Parameters

Several TBM operational variables are missing or incomplete. The grouting volume was not recorded for some tunnel sections; therefore, values estimated by the construction company were used. In Zone 1, the penetration rate was not logged directly and was therefore calculated from the raw data as the ratio of the advancement distance to the excavation time.

- Settlement Assessment in Zone 1

The maximum surface settlements for Zone 1 were manually extracted from the monitoring data provided by the surveying company, VBSS, because the explicit maximum values were not directly recorded. This procedure preserved the data continuity for model training, although it may have introduced minor variability owing to the interpretive nature of manually identifying the maximum values.

- Face Pressure Assessment

The face pressure (earth pressure) was measured using eleven sensors arranged clockwise. Three sensors located near the crown were selected for analysis because of their higher reliability; the other sensors were more prone to malfunction or data distortion caused by soil adhesion or blockage. For future work, we recommend including direct measurements of key geotechnical parameters, such as cohesion (c) and friction angle (φ), to improve soil characterization.

***Final* Remarks** This study highlights the capability of ANNs to predict tunneling-induced settlement with high accuracy. When paired with robust sensitivity analyses, the dual approach combining perturbation-based and weight-based methods bridges the 'black-box' gap by revealing both the model's internal structure and its real-world responsiveness. The findings provide actionable guidance for future urban tunneling operations, especially in soft ground contexts, such as the Algiers Metro. Moving forward, real-time adaptive learning and sensor integration offer promising avenues for enhancing the predictive accuracy and risk management in mechanized tunneling.

AFFILIATIONS AND AUTHOR DETAILS

Corresponding Author

Ilies AYARI – *Undergraduate Author, Department of Civil Engineering, National Polytechnic school of Algiers, Algiers 16200, Algeria;* 0009-0002-9354-9328
Email: ilies.ayari@g.enp.edu.dz

Author

Yacine DERBAL – *Undergraduate Author, Department of Civil Engineering, National Polytechnic school of Algiers, Algiers 16200, Algeria;* 0009-0002-9943-3414
Email: yacine.derbal@g.enp.edu.dz

REFERENCES

(1) The New Arab. Algiers commutes back in time with metro station museum. *The New Arab* (2018). Available at: https://www.newarab.com/features/algiers-commutes-back-time-metro-station-museum

(2) Niu, G., He, X., Xu, H. & Dai, S. Tunneling-induced ground surface settlement: A comprehensive review with particular attention to artificial intelligence technologies. *Nat. Hazards Res.* **4**, 148–168 (2024). https://doi.org/10.1016/j.nhres.2023.11.002

(3) Su, Q., Li, Y., Zhang, Y. & Wang, L. Artificial intelligence–driven tunneling-induced surface settlement prediction: Dataset, feature selection, and model evaluation. *Tunnelling and Underground Space Technology* **167**, 105559 (2024). https://doi.org/10.1016/j.tust.2024.105559

(4) Xu, C., Cao, B. T., Yuan, Y. & Meschke, G. A multi-fidelity deep operator network (DeepONet) for fusing simulation and monitoring data: Application to real-time settlement prediction during tunnel construction. *arXiv preprint* arXiv:2310.00057 (2023). https://doi.org/10.48550/arXiv.2310.00057

(5) Tang, H. & Na, L. Comparison of machine learning methods for ground settlement prediction with different tunneling datasets. *J. Rock Mech. Geotech. Eng.* **13**, 1274–1290 (2021). https://doi.org/10.1016/j.jrmge.2021.08.006

(6) Zhou, S., Zhang, D., Gao, Y. & Zhang, Q. An optimized XGBoost model for predicting tunneling-induced ground settlement. *Sustainability* **16**, 4693 (2024). https://doi.org/10.3390/su16114693

(7) Suwansawat, S. & Einstein, H. H. Artificial neural networks for predicting the maximum surface settlement caused by EPB shield tunneling. *Tunn. Undergr. Space Technol.* **21**, 445–458 (2006). https://doi.org/10.1016/j.tust.2006.01.001

(8) Boubou, F. E. R. & Kastner, R. Artificial neural network application for the prediction of ground surface movements induced by shield tunneling. Can. Geotech. J. 47, 1215–1233 (2010). https://doi.org/10.1139/T10-022

(9) Yaghoubi, E. et al. A systematic review and meta-analysis of artificial neural network, machine learning, deep learning, and ensemble learning approaches in the field of geotechnical engineering. *Neural Comput. Appl.* **36**, 12655–12699 (2024). https://doi.org/10.1007/s00521-024-09893-7

(10) Samek, W., Wiegand, T. & Müller, K.-R. Explainable artificial intelligence: understanding, visualizing and interpreting deep learning models. *arXiv* (2017).

(11) Li, X. et al. Interpretable deep learning: interpretation, interpretability, trustworthiness, and beyond. *arXiv* (2021).

(12) Shao, W. W., Yue, W., Zhang, Y. & Zhou, T. The application of machine learning techniques in geotechnical engineering: a review and comparison. *Math.* (Basel) **11**, (2023). https://doi.org/10.3390/math11183976

(13) Mhatre, S. What is the relation between artificial and biological neuron? *Medium* (2020). Available at: https://saurabhnativeblog.medium.com/what-is-the-relation-between-artificial-and-biological-neuron-18b05831036.

(14) Kim, P. *MATLAB Deep Learning: With Machine Learning, Neural Networks and Artificial Intelligence*. (Apress, Berkeley, CA, 2017). https://doi.org/10.1007/978-1-4842-2845-6

(15) Fahlman, S. E. & Lebiere, C. The Cascade-Correlation Learning Architecture. In *Advances in Neural Information Processing Systems* **2**, 524–532 (Morgan Kaufmann, 1990). Available at: https://papers.nips.cc/paper_files/paper/1990/file/fd6bbf5c96f4df552ed77c3b62c251c4-Paper.pdf

(16) Reed, R. Pruning algorithms—A survey. IEEE Trans. Neural Netw. 4, 740–747 (1993). https://doi.org/10.1109/72.248452